



International Operational Modal Analysis Conference

20 - 23 May 2025 | Rennes, France

Compensating Low Instrumentation for Mode Shape Estimation in Bayesian Filtering with Time-Delayed Data Embedding

Ananay Thakur¹, Shereena O A¹, Subhamoy Sen¹, and Laurent Mevel²

¹ i4S Laboratory, Indian Institute of Technology Mandi, Mandi, HP, India, subhamoy@iitmandi.ac.in

² Univ. Gustave Eiffel, Inria, COSYS-SII, I4S Team, France, laurent.Mevel@inria.fr

ABSTRACT

Reconstructing mode shapes with precision is essential for monitoring structural health, as it provides crucial insights into assessing system integrity. However, challenges like data loss, insufficient and non-collocated instrumentation, and reliance on Finite Element Method-based frameworks or static expansion techniques often lead to decreased accuracy in estimating dynamic characteristics. Some strategies attempt to address data sparsity through spatial virtual sensors—model-predicted responses at unmeasured points—but these reconstructed responses frequently fail to adequately replace real sensor data owing to having been contingent on the prior assumptions on the system's health state. To tackle these issues, this study presents an innovative method that improves the measurement model by incorporating time-lagged measurement layers, enhancing observability for the estimable system states. The model undergoes updates in the time domain via the Interacting Particle Kalman Filter (IPKF) algorithm by embedding time-delayed measurements. This results in more accurate system matrices and refined mode shapes, guaranteeing the accurate reconstruction of key dynamic properties. Numerical tests on a simply supported beam experiencing ambient vibration highlight the proposed method's greater accuracy and computational efficiency than traditional approaches.

Keywords: Virtual Sensor, Mode Shape Reconstruction, Condition monitoring, State estimation, Limited data, Bayesian Filtering.

1. INTRODUCTION

Structural health monitoring (SHM) is indispensable for safeguarding the safety, reliability, and longevity of engineering structures. As modern infrastructure grows increasingly complex, the demand for advanced SHM systems has intensified to facilitate early detection of damage and deterioration, thereby averting catastrophic failures and optimizing maintenance strategies. Despite significant advancements

in SHM, modal parameters continue to serve as a cornerstone for evaluating structural behavior and diagnosing potential damage [1]. These parameters, intrinsically tied to a structure's stiffness and mass, govern its dynamic response to external forces, with variations often signaling the onset of damage or degradation [2, 3]. Among these, mode shapes stand out as a critical diagnostic tool, offering high-resolution spatial insights into vibrational behavior. Their pronounced sensitivity to changes in stiffness and mass renders them indispensable for pinpointing localized damage, diagnosing structural anomalies, and refining computational models to reflect real-world conditions with precision [4].

Estimating and reconstructing mode shapes with precision poses considerable technical difficulties, especially in practical settings [5]. Challenges such as limited sensor coverage, data noise, and structural changes from environmental effects, aging, or damage undermine the effectiveness of conventional methods. Techniques like the Finite Element Method (FEM) or static expansion typically depend on strict structural assumptions, challenging to maintain in varying operational conditions [6, 7]. Although successful in controlled settings, these methods often inadequately address real-world structural dynamics, causing inaccuracies in damage detection and health monitoring.

Accordingly, an alternative strategy in SHM involves the deployment of Virtual Sensors (VS), which estimate responses at uninstrumented locations based on predefined structural models. While this approach shows promise [8], its effectiveness is limited by the accuracy of the underlying model. Discrepancies between the model and the actual structure can result in significant errors, particularly in scenarios where the structural properties deviate from their assumed baseline.

To address these inherent limitations, this study proposes a novel methodology that leverages time-lagged measurements for enhanced mode shape reconstruction. Unlike conventional approaches, the proposed method integrates temporally shifted response data into the system model, thereby enhancing the observability of dynamic properties without relying solely on spatial interpolation or strong model assumptions. The methodology employs the Interacting Particle Kalman Filter (IPKF), a filtering algorithm for dynamic system estimation, enabling precise and computationally efficient updating of system matrices in the time domain. This innovative approach facilitates robust modal parameter estimation, especially in the presence of sparse data.

2. METHODOLOGY

A Linear Time-Invariant (LTI) dynamic system of order n can be represented by the following governing equation:

$$\mathbf{M}\ddot{\mathbf{q}}(t) + \mathbf{C}\dot{\mathbf{q}}(t) + \mathbf{K}\mathbf{q}(t) = \mathbf{P}(t) \quad (1)$$

where $\mathbf{q}(t)$, $\dot{\mathbf{q}}(t)$, and $\ddot{\mathbf{q}}(t)$ represent the system's displacement, velocity, and acceleration response vectors, respectively, under the influence of an external excitation force vector $\mathbf{P}(t)$. The stiffness matrix (\mathbf{K}), the mass matrix (\mathbf{M}), and the damping matrix (\mathbf{C}) are assumed to be time-invariant and of order $n \times n$.

This work evaluates the efficacy of Bayesian filtering techniques for state estimation in scenarios with limited observational data, employing a delay-embedded measurement model. Since practical systems produce discrete-time data, the continuous-time dynamics must be represented in discrete-time state-space form, as shown in Equation (2). This requires the initial formulation of the continuous-time state-space representation, followed by the discretization of the system matrices to derive (\mathbf{A} , \mathbf{B} , \mathbf{H} , and \mathbf{G}). A comprehensive derivation of these matrices can be found in [9].

$$\begin{aligned} \text{Process equation:} \quad \mathbf{x}_k &= \mathbf{A}_k \mathbf{x}_{k-1} + \mathbf{B}_k \mathbf{f}_k + \mathbf{w}_k \\ \text{Measurement equation:} \quad \mathbf{y}_k &= \mathbf{H}_k \mathbf{x}_k + \mathbf{G}_k \mathbf{f}_k + \mathbf{v}_k \end{aligned} \quad (2)$$

where \mathbf{x}_k is the discrete-time state vector of the order $(2n \times 1)$ consisting of displacements and velocities corresponding to each of the n degrees of freedom (*dofs*). The vector \mathbf{f}_k represents the external excitation of size $n \times 1$, modeled as a Stationary White Gaussian Noise (SWGN) process with a specified covariance. The observation vector \mathbf{y}_k , of dimension $m \times 1$, contains the system's measured outputs.

The matrices $\mathbf{A}_k \in \mathbb{R}^{2n \times 2n}$, $\mathbf{B}_k \in \mathbb{R}^{2n \times n}$, $\mathbf{H}_k \in \mathbb{R}^{m \times 2n}$, and $\mathbf{G}_k \in \mathbb{R}^{m \times n}$ denote the discrete-time state transition, input, observation, and direct transmission matrices, respectively. The stochastic processes \mathbf{w}_k and \mathbf{v}_k represent process noise and measurement noise, which are modeled as SWGN with covariances \mathbf{Q} and \mathbf{R} , respectively.

Bayesian filtering algorithms are employed to address the state estimation problem for the above class of linear stochastic systems. However, these inverse stochastic estimation approaches are inherently ill-posed and rely on sufficient observation data. Limited data availability due to inaccessibility to instrumentation, malfunction, or data loss degrades system observability and, consequently, the performance of traditional filtering methods. In damage quantification and localization problems, the lack of observation data hinders the performance of traditional state parameter estimation algorithms.

However, reconstructing dynamic responses at unobserved locations can enhance the SHM techniques. Delay embedding increases the effective size of the measurement model, and thereby available external observable information is fed into the model, compensating for the ill-posedness. Therefore, the current study explores the applicability of delay embedding to mitigate the challenges associated with data sparsity, potentially improving both precision and accuracy without additional costs.

Spatial VS addresses data sparsity by utilizing a supporting model to reconstruct responses at locations where data is absent. The method's accuracy hinges on the supporting model's quality, and using high-dimensional models may cause estimation delays. This research, however, presents an approach that integrates both current and delayed data for state observation. By including delayed virtual measurements, the method resolves issues of ill-posedness due to data sparsity, facilitating effective reconstruction of unobserved responses. A delay-embedded measurement vector is created by enhancing observation data with delayed or future measurements.

The number of delay layers, denoted by z , if sufficient, guarantees system observability and extends beyond the sensor layer. Delayed measurement vectors represent extended observations for the current state vector \mathbf{x}_k . According to the system dynamics in Equation (2), the observation at $k + 1$, \mathbf{y}_{k+1} , can be expressed as:

$$\mathbf{y}_{k+1} = \mathbf{H}_{k+1}\mathbf{x}_{k+1} + \mathbf{G}_{k+1}\mathbf{f}_{k+1} + \mathbf{v}_{k+1} \quad (3)$$

Which, through substituting \mathbf{x}_{k+1} from Equation (2), renders as:

$$\mathbf{y}_{k+1} = [\mathbf{H}_{k+1}\mathbf{A}_{k+1}]\mathbf{x}_k + [\mathbf{H}_{k+1}\mathbf{B}_{k+1} + \mathbf{G}_{k+1}]\mathbf{f}_{k+1} + \mathbf{H}_{k+1}\mathbf{w}_{k+1} + \mathbf{v}_{k+1} \quad (4)$$

The approach can further be expanded to generate observations for \mathbf{x}_k as \mathbf{y}_{k+2} , \mathbf{y}_{k+3} and further. Sequential observations stored in an augmented measurement vector $\bar{\mathbf{y}}_k \in \mathbb{R}^{(z+1)m}$, given by $\bar{\mathbf{y}}_k = [\mathbf{y}_k^T \ \mathbf{y}_{k+1}^T \ \dots \ \mathbf{y}_{k+z}^T]^T$ enhances the observability aspect for the states and consequently its estimation. As per Takens' theorem [10], $(z + 1)m > 2n + 1$ ensures complete observability and reconstruction of the states. For simplicity, the measurement equation when $z = 2$ is:

$$\bar{\mathbf{y}}_k = \begin{bmatrix} \mathcal{H}_k & \vdots & \mathcal{G}_k \end{bmatrix} \begin{bmatrix} \mathbf{x}_k \\ \mathbf{f}_k \end{bmatrix} + \mathcal{W}_k \bar{\mathbf{w}}_k + \bar{\mathbf{v}}_k \quad (5)$$

where,

$$\begin{aligned} \mathcal{H}_k &= \begin{bmatrix} \mathbf{H}_k \\ \mathbf{H}_{k+1}\mathbf{A}_{k+1} \\ \mathbf{H}_{k+2}\mathbf{A}_{k+2}\mathbf{A}_{k+1} \end{bmatrix}, \quad \mathcal{G}_k = \begin{bmatrix} \mathbf{G}_k & \mathbf{0} & \mathbf{0} \\ \mathbf{0} & \mathbf{H}_{k+1}\mathbf{B}_{k+1} + \mathbf{G}_{k+1} & \mathbf{0} \\ \mathbf{0} & \mathbf{H}_{k+2}\mathbf{A}_{k+2}\mathbf{B}_{k+1} & \mathbf{H}_{k+2}\mathbf{B}_{k+2} + \mathbf{G}_{k+2} \end{bmatrix}, \\ \mathcal{W}_k &= \begin{bmatrix} \mathbf{0} & \mathbf{0} & \mathbf{0} \\ \mathbf{0} & \mathbf{H}_{k+1} & \mathbf{0} \\ \mathbf{0} & \mathbf{H}_{k+2}\mathbf{A}_{k+2} & \mathbf{H}_{k+2} \end{bmatrix}. \end{aligned} \quad (6)$$

Combining Equations (2) and (5), the augmented discrete-time state-space formulation is:

$$\begin{aligned} \mathbf{x}_k &= \mathbf{A}_k \mathbf{x}_{k-1} + \mathbf{B}_k \bar{\mathbf{f}}_k + \tilde{\mathbf{w}}_k \\ \bar{\mathbf{y}}_k &= \mathcal{H}_k \mathbf{x}_k + \mathcal{G}_k \bar{\mathbf{f}}_k + \tilde{\mathbf{v}}_k \end{aligned} \quad (7)$$

where, $\mathcal{B}_k = [\mathbf{B}_k \quad \mathbf{0} \quad \mathbf{0}]$, $\tilde{\mathbf{w}}_k = [\mathbf{I} \quad \mathbf{0} \quad \mathbf{0}] \bar{\mathbf{w}}_k$, $\tilde{\mathbf{v}}_k = \mathcal{W}_k \bar{\mathbf{w}}_k + \bar{\mathbf{v}}_k$.

The process noise $\tilde{\mathbf{w}}_k$ and measurement noise $\tilde{\mathbf{v}}_k$ are characterized by covariances $\tilde{\mathbf{Q}}_k$ and $\tilde{\mathbf{R}}_k$, respectively. While detailed derivations of these covariances are omitted for brevity.

The IPKF framework is employed for estimating the system's state and parameters leveraging sparse measurement data. In the context of the system defined by Equation (7), both the system states and measurements are augmented with additional parameters that characterize the spatially varying health parameters of the system. These health parameters influence the system's physical matrices, i.e., \mathbf{K} , \mathbf{M} , and \mathbf{C} which subsequently affect the system's dynamic behavior. The estimation of these health parameters is performed concurrently with the state vector \mathbf{x}_k , within an integrated filtering approach. The state vector \mathbf{x}_k is estimated using a Kalman Filter, while the health parameters are estimated through a Particle Filter (PF), enabling the simultaneous estimation of both state and health variables in a probabilistic framework.

With the augmented discrete-time state-space representation derived, mode shapes estimation focuses on identifying the system's modal properties encapsulated in the \mathbf{A}_k and \mathbf{H}_k . To enhance the accuracy of modal property estimation, the delay-embedded measurement model is utilized, providing a richer dataset by leveraging temporal correlations across multiple time steps.

To extract mode shapes, the system dynamics are analyzed through modal decomposition, which involves solving the eigenvalue problem for the \mathbf{A}_k , i.e. $\mathbf{A}_k \bar{\Phi}_k = \bar{\Phi}_k \Lambda_k$, where $\bar{\Phi}_k$ is the modal matrix containing eigenvectors (mode shapes) and Λ_k is a diagonal matrix of eigenvalues at time k , corresponding to the system's natural frequencies and damping characteristics. In this analysis, \mathbf{A}_k is assumed to be parameterized by the parameter ξ_k , such that $\mathbf{A}_k = \mathbf{A}(\xi_k)$. This assumption ensures that \mathbf{A}_k reflects the system's true dynamics at each time step. The observable mode shape ϕ_i^k is obtained, for the i -th mode, as $\phi_i^k = \mathbf{H}_k \Phi_k^i$, where Φ_k^i represents the i -th eigenvector of \mathbf{A}_k . To ensure scale invariance and facilitate comparison between mode shapes, normalization is applied to the extracted mode shapes. This step standardizes the results, making them suitable for interpretation and further analysis.

3. NUMERICAL EXPERIMENTS

This research thoroughly examines a simply supported beam to assess the VS-IPKF framework's efficacy in mode shape reconstruction. The beam is divided into 10 elements of equal length (M_1 to M_{10}), each with two nodes. Internal nodes feature two *dofs*: one translational and one rotational. Boundary support nodes include rotational *dofs* only, amounting to 11 nodes and 20 *dofs* in total. Element M_1 is at the left support, and M_{10} is near the right support. This study tests the framework's precision in various

Algorithm 1 Mode Shape Estimation with IPKF for State Estimation

```
1: procedure IPKF( $\bar{\mathbf{y}}_k, \mathbf{Q}, \mathbf{R}$ )
2:   Initialize:
3:     Particles  $\{\xi_0^j\}$ , state estimates  $\{\mathbf{x}_0^j\}$ , state covariance matrix  $P_0$  and weights  $w_0^j = \frac{1}{N_p}$ .
4:   for each time step  $k$  do
5:     procedure PARTICLE EVOLUTION( $\{\xi_{k-1}^j\}, \{\mathbf{x}_{k-1|k-1}^j\}$ )
6:       for each particle  $j=1$  to  $N_p$  do
7:         Evolve parameter:  $\xi_k^j \leftarrow \alpha \xi_{k-1}^j + \mathcal{N}(0, \sigma_k^\xi)$ 
8:       end for
9:     end procedure
10:    procedure KALMAN FILTER( $\{\xi_k^j\}, \{\mathbf{x}_{k-1|k-1}^j\}, \bar{\mathbf{y}}_k$ )
11:      for each particle  $\xi_k^j$  do
12:        Define system matrices:  $\mathbf{A}_k^j = \mathbf{A}(\xi_k^j), \mathbf{H}_k^j = \mathbf{H}(\xi_k^j)$ 
13:        Prediction:  $\mathbf{x}_{k|k-1}^j = \mathbf{A}_k^j \mathbf{x}_{k-1|k-1}^j$ 
14:        Innovation:  $\epsilon_k^j = \bar{\mathbf{y}}_k - \mathbf{H}_k^j \mathbf{x}_{k|k-1}^j$ 
15:        Calculate the Innovation Covariance ( $\mathbf{S}_k^j$ ), and Kalman Gain ( $\mathbf{K}_k^j$ )
16:        Calculate the Predicted State Covariance ( $\mathbf{P}_{k|k-1}^j$ )
17:        State Update:  $\mathbf{x}_{k|k}^j = \mathbf{x}_{k|k-1}^j + \mathbf{K}_k^j \epsilon_k^j$ 
18:        Covariance Update:  $\mathbf{P}_{k|k}^j = (\mathbf{I} - \mathbf{K}_k^j \mathbf{H}_k^j) \mathbf{P}_{k|k-1}^j$ 
19:      end for
20:    end procedure
21:    procedure PARTICLE RESAMPLING( $\{\xi_k^j\}, \bar{\mathbf{y}}_k$ )
22:      for each particle  $\xi_k^j$  do
23:        Weight update:  $w_k^j \propto$  Likelihood of  $\bar{\mathbf{y}}_k$  given  $\xi_k^j$ 
24:      end for
25:      Normalize weights:  $w_k^j = w_k^j / \sum_j w_k^j$ 
26:      Resample particles: Draw  $\xi_k^j$  based on  $w_k^j$ 
27:    end procedure
28:    Calculate state estimates:  $\mathbf{x}_{k|k} = \sum_j w_k^j \mathbf{x}_{k|k}^j$ 
29:    Calculate parameter estimates:  $\xi_k = \sum_j w_k^j \xi_k^j$ 
30:  end for
31: end procedure
32: procedure MODE SHAPE ESTIMATION
33:   Define  $\mathbf{A}_k = \mathbf{A}(\xi_k)$  and  $\mathbf{H}_k = \mathbf{H}(\xi_k)$ .
34:   Solve eigenvalue problem:  $\mathbf{A}_k \Phi_k = \Phi_k \Lambda_k$ 
35:   Output: Eigenvalues  $\Lambda_k$ , Eigenvectors  $\Phi_k$ , and mode shapes  $\phi_k = \mathbf{H}_k \Phi_k$ 
36: end procedure
```

scenarios, offering insights into its effectiveness for structural health monitoring. The following sections detail the examined cases.

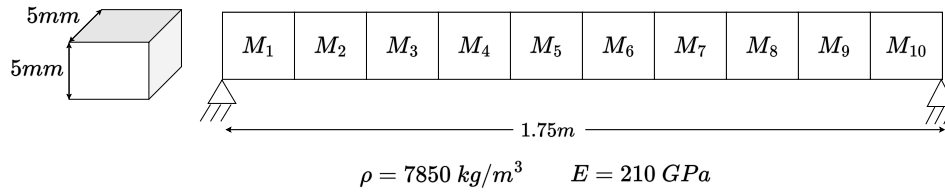


Figure 1: Geometry and details of the simply supported beam

3.1. Reconstruction of Mode Shapes Under Healthy Conditions

This research assesses the precision in reconstructing mode shapes of an intact structure utilizing the VS-IPKF framework. The mode shapes from the FEM healthy model are used as a reference for comparison against those reconstructed via the VS-IPKF framework and those obtained via the Stochastic Subspace Identification (SSI) technique. This foundational study demonstrates the VS-IPKF framework's proficiency in accurately capturing mode shapes under optimal, undamaged conditions. Notice that thanks to the increase in the layer count z , the total number of sensors (virtual or not) is always 20. That is why the results on the right are similar, whereas they decrease in quality on the left.

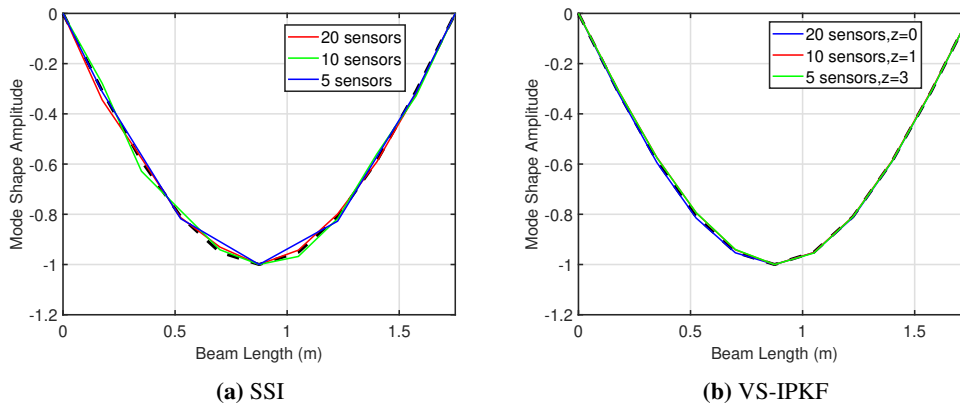


Figure 2: Reconstructed Mode Shape for Healthy Structure (*dashed line represents the FEM mode*)

3.2. Reconstruction Accuracy Under Structural Damage

Next, this subsection investigates the effectiveness of the VS-IPKF framework in reconstructing mode shapes in the presence of unknown estimated structural damage. Damage is modeled by systematically reducing the stiffness of specific elements in the structure. This analysis highlights the framework's ability to estimate variations in structural properties while maintaining high reconstruction accuracy.

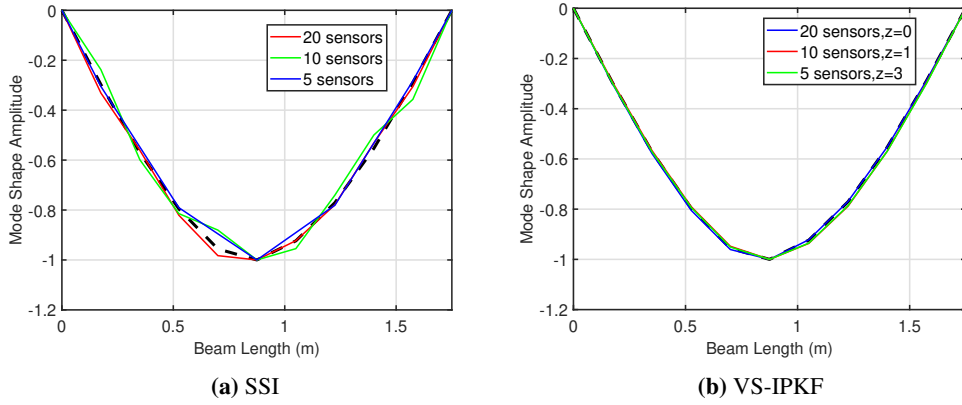


Figure 3: Mode Shape Reconstruction Under Damage (*dashed line represents the FEM mode*)

3.3. Robustness Under Sparse Sensor Configuration

The robustness of the VS-IPKF framework under sparse measurement conditions is evaluated by reducing the number of physical sensors deployed along the beam to 5. The reconstructed mode shapes from the VS-IPKF framework, along with the Modal Assurance Criterion (MAC), are compared for different values of z , from $z = 0$ to 3, providing insights into the trade-off between reconstruction accuracy and reduced measurement configurations. This evaluation underscores the framework’s effectiveness in achieving accurate reconstructions despite limited physical measurements, demonstrating its potential for resource-constrained settings.

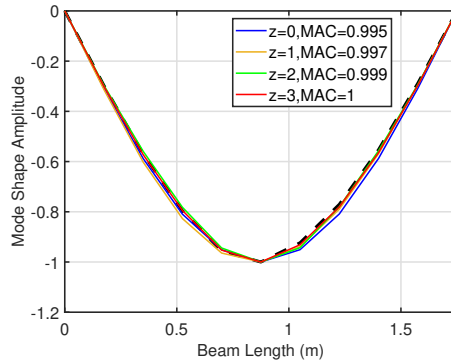


Figure 4: Mode Shape reconstruction of 5 sensors for different layer choices

The MAC between the estimated mode shape and its FEM counterpart goes to 1 with increasing z .

4. DISCUSSION AND CONCLUSION

Notice that SSI was selected as a comparison method to our proposed VS-IPKF approach since it shares the same property of stacking time-lagged measurements in building its Hankel data matrices. The comparatively superior behavior of our approach on non-measured points comes from the mixing of both a model and time-lagged measurement, whereas SSI is purely data-driven and as such only relies on the time-lagged measurements. Notice that virtual spatial sensors rely only on the model and are expected to behave worse than VS-IPKF, an assumption that will be verified in a companion paper.

Within VS-IPKF, The delay-embedded framework VS enhances modal estimation by improving space resolution and robustness compensating for data sparsity, whereas the IPKF part estimates simultaneously damage changes. The limits of this approach for detecting localized stiffness changes with small instrumentation will be tested regarding model complexity and real-life robustness later on.

ACKNOWLEDGMENTS

This research was partially funded by the Aeronautics Research and Development Board, New Delhi, India, through grant file no. ARDB/01/1052042/M/I.

REFERENCES

- [1] C. R. Farrar and K. Worden. An introduction to structural health monitoring. *Philosophical Transactions of the Royal Society A: Mathematical, Physical and Engineering Sciences*, 365(1851):303–315, 2007. doi: 10.1098/rsta.2006.1928.
- [2] George Hearn and Rene B Testa. Modal analysis for damage detection in structures. *Journal of structural engineering*, 117(10):3042–3063, 1991.
- [3] Maciej Radziński, Marek Krawczuk, and Magdalena Palacz. Improvement of damage detection methods based on experimental modal parameters. *Mechanical Systems and Signal Processing*, 25(6):2169–2190, 2011. ISSN 0888-3270. doi: <https://doi.org/10.1016/j.ymsp.2011.01.007>. URL <https://www.sciencedirect.com/science/article/pii/S0888327011000173>. Interdisciplinary Aspects of Vehicle Dynamics.
- [4] Chunwei Zhang, Asma A. Mousavi, Sami F. Masri, Gholamreza Gholipour, Kai Yan, and Xiuling Li. Vibration feature extraction using signal processing techniques for structural health monitoring: A review. *Mechanical Systems and Signal Processing*, 177:109175, 2022. ISSN 0888-3270. doi: <https://doi.org/10.1016/j.ymsp.2022.109175>. URL <https://www.sciencedirect.com/science/article/pii/S0888327022003326>.
- [5] Maria Giovanna Masciotta and Daniele Pellegrini. Tracking the variation of complex mode shapes for damage quantification and localization in structural systems. *Mechanical Systems and Signal Processing*, 169:108731, 2022.
- [6] Marius Tarpø, Bruna Nabuco, Christos Georgakis, and Rune Brincker. Expansion of experimental mode shape from operational modal analysis and virtual sensing for fatigue analysis using the modal expansion method. *International Journal of Fatigue*, 130:105280, 2020. ISSN 0142-1123. doi: <https://doi.org/10.1016/j.ijfatigue.2019.105280>. URL <https://www.sciencedirect.com/science/article/pii/S0142112319303846>.
- [7] Hua-Peng Chen, Kong Fah Tee, and Yi-Qing Ni. Mode shape expansion with consideration of analytical modelling errors and modal measurement uncertainty. *Smart structures and systems*, 10(4-5):485–499, 2012.
- [8] O. A. Shereena, Subhamoy Sen, and Laurent Mevel. Mitigating ill-posedness in parameter estimation under sparse measurement for linear time-varying systems employing virtual sensor responses. In *Proceedings of the 11th European Workshop on Structural Health Monitoring (EW-SHM 2024)*, pages 1–11, Potsdam, Germany, June 2024. NDT.net. doi: 10.58286/29673. URL <https://inria.hal.science/hal-04651217>.
- [9] Subhamoy Sen, Antoine Crinière, Laurent Mevel, Frédéric Cérou, and Jean Dumoulin. Seismic-induced damage detection through parallel force and parameter estimation using an improved interacting particle-kalman filter. *Mechanical Systems and Signal Processing*, 110:231–247, 2018. ISSN 0888-3270. doi: 10.1016/j.ymsp.2018.03.016.
- [10] Cosma Rohilla Shalizi. *Methods and Techniques of Complex Systems Science: An Overview*, pages 33–114. Springer US, Boston, MA, 2006. ISBN 978-0-387-33532-2. doi: 10.1007/978-0-387-33532-2.2. URL https://doi.org/10.1007/978-0-387-33532-2_2.